

# Linewidth reduction by 6 orders of magnitude of a broad-area 729-nm diode laser

Marie Houssin, Philippe Courteille, Caroline Champenois, Mustapha Herbane, Martina Knoop, Michel Vedel, and Fernande Vedel

Diode lasers with a power output superior to 100 mW are in widespread use in medical as well as research applications. However, for such diodes lasing oscillation generally occurs simultaneously in several longitudinal and transverse modes that are unsuitable for high-resolution spectroscopy. We spectrally narrow a 100-mW broad-area diode laser by first using an extended cavity and then an electrical feedback produced by a Pound–Drever–Hall stabilization on a low-finesse reference cavity. Reduction of the linewidth by more than 6 orders of magnitude is achieved (the output linewidth is narrowed from 1 THz to less than 500 kHz), making possible its use for high-resolution spectroscopy. The power and the spectral qualities of this diode laser allow us to induce quantum jumps toward the  $D_{5/2}$  metastable level of single  $\text{Ca}^+$  ions. © 2003 Optical Society of America

OCIS codes: 140.0140, 140.2020, 140.5960, 300.3700.

## 1. Introduction

Stable and spectrally narrow lasers are essential for high-resolution spectroscopy, optical frequency standards, and many fundamental experiments in physics.<sup>1</sup> In the past, dye lasers have been extensively used for spectroscopy because of their wide tuning range, spectral purity, and high power. Today the use of diode lasers is attractive because they are compact, inexpensive, and require low power. The major drawback is the limited availability of diode lasers for specific wavelengths that are imposed by the energy levels of the atom under investigation. The given wavelength domains generally correspond to different manufacturing technologies.

Our current project consists of building an optical frequency standard that involves a single cold  $\text{Ca}^+$  ion confined in a miniature radio-frequency trap. The 411-THz frequency of the clock transition (between the fundamental  $4S_{1/2}$  state and the metastable  $3D_{5/2}$  state) corresponds to a 729-nm wavelength.<sup>2,3</sup>

The natural linewidth of this electric quadrupole transition is less than 1 Hz. The possible subkilohertz linewidth of the atomic spectral profile can be reached by Doppler laser cooling into the Lamb–Dicke regime. For this purpose, three wavelengths are required: 729 nm for the clock transition, 397 nm for the strong cooling transition, and 866 nm for repumping the atoms that decay from the upper level ( $4P_{1/2}$ ) of the cooling transition into the metastable  $3D_{3/2}$  state. All these wavelengths can be generated by diode lasers. For the clock transition, the only powerful diode laser available at this time is a broad-area laser (BAL), which is normally used in near-infrared reflectance spectroscopy for medical applications.<sup>4</sup> This diode laser is available with a nominal output power of as much as 250 mW. The free running emitted light is multimode, spatially as well as spectrally, with a nominal linewidth of 2 nm (1.1 THz).

Here we report on the improvement of the spectral and spatial properties of the above diode laser. Indeed, frequency and mode qualities of diode lasers are different for various types of laser and wavelength, the manner and the strategy to achieve the best performance must be found for each new diode setup.

First we show how to obtain a spectrally single-mode emission by placing the BAL in an extended cavity. We then describe the shaping of the spatial profile and the optical setup to correct the laser beam astigmatism to within a level that allows good injection into a single-mode optical fiber. Next we de-

All the authors are with Physique des Interactions Ioniques et Moléculaires, Unite Mixte de Recherche 6633, Centre National de la Recherche Scientifique, Université d'Aix-Marseille 1, Centre de St. Jérôme, Case C21, F-13397 Marseille Cedex 20, France. The e-mail address for M. Houssin is mhoussin@up.univ-mrs.fr.

Received 6 January 2003; revised manuscript received 9 May 2003.

0003-6935/03/244871-06\$15.00/0

© 2003 Optical Society of America

scribe the first stage of frequency stabilization of the diode by means of an electronic feedback loop, for which the frequency reference is a stable optical cavity with a finesse of 300 and mounted on an Invar rod. Finally, to test the performance of this BAL laser setup, we used it to induce quantum jumps with  $\text{Ca}^+$  ions.

## 2. Extended Cavity Setup

The diode investigated in this study is an AOC 730-100-TO3 BAL from Applied Optronics Corporation<sup>5</sup> that emit 100 mW for a current of 780 mA and a temperature of 25 °C at 728 nm. This BAL consists of a single quantum well structure made by metal-organic chemical-vapor deposition. Its typical junction size is 100  $\mu\text{m}$   $\times$  1  $\mu\text{m}$ . The measured divergence of the emitted spatially multimode light is approximately 8° in the plane parallel to the height of the junction and 38° in the perpendicular direction. When the free-running laser functioned at a power of 100 mW, the spectral width was approximately 2 nm.

To obtain single-mode emission at 729 nm and to tune the wavelength to the resonance of the atomic transition we set the diode into an external cavity.<sup>6,7</sup> The diode was temperature stabilized at 17 °C with an uncertainty of less than 0.02 °C/day. At this temperature the threshold current of the free-running diode was 580 mA. Collimation of the light emitted from the diode was obtained with an aspherical lens of 6.3-mm focal length, the clear aperture was 5 mm, and the numerical aperture was 0.4. The extended cavity had a 2400-grooves/mm grating mounted in a Littrow configuration. The 44-nm cavity length corresponded to a 3.4-GHz free-spectral range. The temperature of the base plate of the laser was controlled to a 0.02 °C resolution that minimizes thermal drifts of the cavity length. The grating was mounted so its grooves were vertical, that is, parallel to the larger dimension of the junction. The number of illuminated grooves was then maximum and yielded an optimized resolution. The measured grating efficiency was equal to 22% in the first diffraction order. The spectral width of the light, which was diffracted by the grating and fed back into the 1- $\mu\text{m}$  large junction, was estimated from geometric parameters to be approximately 40 GHz. The output beam of this laser corresponds to a zero order with 50% measured efficiency. The grating was mounted on a piezoelectric transducer (PZT) whose displacement is 6 nm/V. It permits a longitudinal adjustment of the cavity length corresponding to a continuous frequency tuning of 56 MHz/V. The output beam linewidth measured with a 10-cm-long Fabry-Perot analyzer (with a measured finesse of 300) was found to be 8 MHz.

Since setting a laser diode in an extended cavity lowers its threshold current, we adjusted the grating feedback by minimizing the threshold. With optimal adjustment, we could obtain a 28% reduction of the threshold current from 580 to 420 mA. In a previous experiment, when Pawletko *et al.* studied the injection of a 796-nm BAL diode with a single-

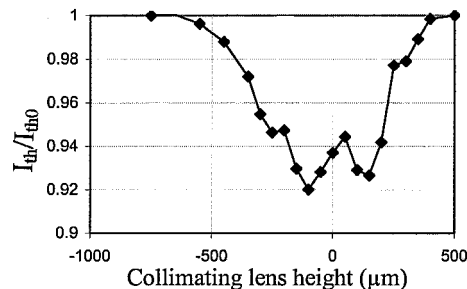


Fig. 1. Measured current threshold ( $I_{th}$ ) normalized to the free-running diode threshold ( $I_{th0}$ ) when the diode is placed in an extended cavity versus the vertical position of the collimating lens. A 100- $\mu\text{m}$  displacement of the lens corresponds to a variation of 0.9° of the injection angle of the feedback beam. (These operating conditions did not allow us to reach optimal threshold current reductions.)

mode laser, they observed a critical dependence of the optimized adjustment on physical and geometric parameters,<sup>8</sup> one of which is the value of the injection angle. Because of the degradation of the near-field output that is due to filamentation in large optical cavities,<sup>9,10</sup> the injected beam must present a small angle with the plane that contains the large dimension of the strip to ensure full saturation of the whole region of the chip. In a similar way, in the present research we observed two minima for the threshold current while moving the collimating lens along the vertical direction (Fig. 1). We can explain this effect by considering that grating feedback can be understood as a self-injection process. These two optimized positions correspond to two symmetric angles of injection versus the emission axis. These angles were measured to be  $\pm 2.2^\circ$ . The slight asymmetry of the curve in Fig. 1 comes from a small misalignment of the whole assembly (diode, collimating lens, grating) and a spatial inhomogeneity of the laser junction.

In a pure extended cavity in which the output facet of the diode is antireflection coated, the laser cavity is the total cavity formed by the end facet of the diode and the grating. In our setup, the nominal reflectivity of the output facet of the diode is approximately 3%. The field inside the laser diode chip is the superposition of the field reflected by the output facet of the diode with the field reflected by the grating. The resulting interferences influence the emitted power and the frequency behavior.<sup>11</sup> The setup behaves as a two-coupled-cavity device.<sup>12</sup> When we tuned the emitted frequency by sweeping the injection current or the voltage that is applied to the PZT of the grating mount, variation of the output power of the extended cavity versus the current intensity caused modulation as shown in Fig. 2. This modulation results from the phase difference in the two internal fields induced by the current variation. In Fig. 2 upper levels of the output power correspond to intervals in which the diode laser is single mode. Between two single-mode regimes, mode hops appear. When increasing the laser current above the threshold ( $I =$

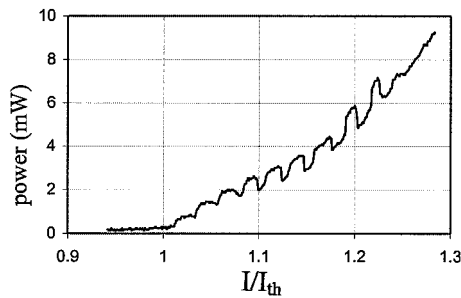


Fig. 2. Output laser power versus the laser injection current (normalized to the threshold current  $I_{th}$ ) when the diode was placed into an extended cavity.

420 mA) from a single-mode regime, the laser first oscillates on two modes with a mode difference of 3.4 GHz, which corresponds to the free spectral range of the extended cavity. Then the diode laser operates in a multimode regime. With an increase in current, the single-mode tuning range is narrowed. For a current  $I$  with a value of  $480 \text{ mA} < I < 570 \text{ mA}$ , the laser works in a quasi-single-mode regime of the extended cavity, in spite of the presence of a small peak at the nearest mode of this cavity. Indeed, the selectivity of the grating is not sufficient. For higher values ( $I > 570 \text{ mA}$ , which is the free-running diode threshold), the laser operates definitively in a multimode way, as a consequence of competition between the diode cavity emission and the extended cavity emission. In the single-mode operation, the usual value of the continuous tuning range, when either the PZT voltage or the current varies is 1.6 GHz (50% of the free spectral range). The value increases to 3.5 GHz when a suitable combination of PZT voltage and diode current variations is chosen. At  $I = 480 \text{ mA}$ , the single-mode power at the output of the laser is approximately 7.7 mW at  $\lambda \approx 729.4 \text{ nm}$ . Less than 10% of the nominative power of the free-running diode is obtained in a single-mode regime. Also taking into account the necessary use of power for frequency stabilization of the laser, our setup requires the use of high-power semiconductor components.

Using an extended cavity will also improve the spatial properties of the laser. A comparison of the laser beam intensity profiles in the direction of the long dimension of the laser junction in the near field without and with feedback causes a width reduction of the emitting area. This reduction makes the emission single mode as confirmed by the Gaussian far-field profile. Along the small direction of the junction, the far-field profile is almost nearly Gaussian but its divergence before collimation is large because of the small size of the junction and therefore the ellipticity of the emission is approximately 7. To increase the power of the laser in the center of the beam, we put a slit inside the cavity. The slit of various widths, vertical and parallel to the large size of the junction, was placed close to the collimating lens between this lens and the grating, in a place in which the beam is nearly collimated. The slit acts as a diaphragm that reduces the horizontal dimension of

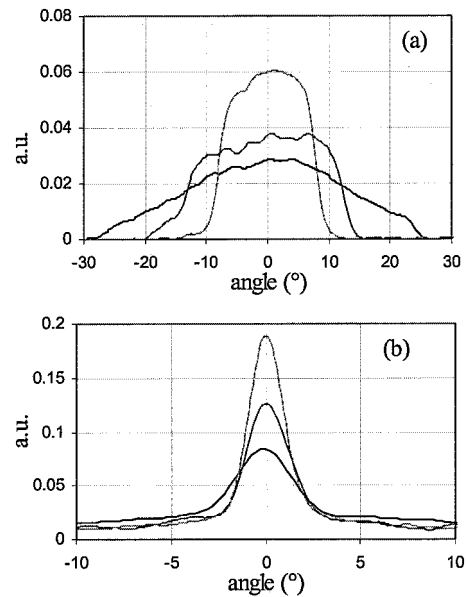


Fig. 3. Far-field profiles of the extended-cavity emission for different slit sizes placed vertically, parallel to the junction inside the cavity. Intensity distribution (a) normal to the junction plane and (b) in the junction plane. Bottom curve, without a slit; middle curve, with a 3-mm-wide slit; top curve, with a 2-mm-wide slit.

the transverse profile [Fig. 3(a)] and therefore modifies the frequency selectivity of the feedback. This allows an increase of the maximum current at which single-mode operation is still possible. Vertically, the power in the profile pedestal is much more important than for classical diodes (60% of the total power). With the slit, a part of the optical power contained in the pedestal is concentrated in the Gaussian lobe [Fig. 3(b)]. However, with a 2-mm slit that gave the best results, 40% of the total power was still in the pedestal. With a 2-mm slit, the threshold current increased to  $I = 460 \text{ mA}$  and the last regime of single-mode operation was reached for  $I = 560 \text{ mA}$  corresponding to a 6.2-mW power at  $\lambda \approx 729.1 \text{ nm}$ . The spatial filtering in the horizontal direction reduces the ellipticity of the emission by a factor of approximately 2.

### 3. Reduction of the Astigmatism

To characterize the astigmatism of the free-running diode, the position of the junction images corresponding to both transverse directions must be known. Moving the collimating lens along the optical axis while seeking the two images in a given plane, allows us to estimate 1.1-mm astigmatism of the diode. As a consequence, when the diode is mounted in an extended cavity and in the case of an optimized feedback coupling, the output of the laser is observed to be collimated in the horizontal direction (perpendicular to the junction and the grating grooves) and divergent in the vertical direction.

To inject the laser beam into a Fabry–Perot cavity or into an optical fiber, we must correct this astigmatism and make the spatial profile circular. We prepared and then set up two different afocal systems for

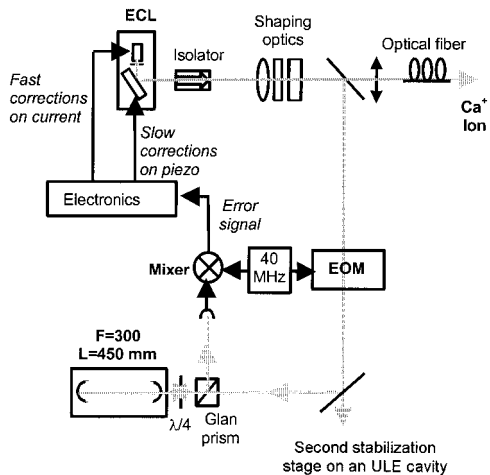


Fig. 4. Optical setup for frequency stabilization: ECL, extended-cavity laser; EOM, electro-optic modulator.

the two main axes. Each system was composed of a common spherical lens (of 100-mm focal length) and a proper cylindrical lens. The focal length of the cylindrical lens in the horizontal direction is 30 mm to reduce the waist size by a factor of 3. The focal length of the cylindrical lens in the vertical direction was 100 mm to conserve the waist size. We adjusted the lens distance to compensate for the beam divergence. The output of the setup is a nearly Gaussian circular beam with an 0.8-mrad divergence.

After this beam optimization, we injected the light into a single-mode optical fiber. The coupling efficiency is representative of the purity of the beam profile. We injected approximately 46% of the light power into the fiber. Under typical conditions, when an important part of the power is lost in the isolator and by reflection on the faces of the various beam-shaping and focusing lenses, we focused 450  $\mu$ W of emergent optical power into a 50- $\mu$ m waist.

#### 4. Stabilization to a Reference Cavity

The linewidth of the extended-cavity laser is approximately 8 MHz depending on the laser power. Locking the laser frequency to the eigenfrequency of an optical reference cavity allows us to reduce further the laser spectral linewidth. For this goal, we used a Pound–Drever–Hall technique.<sup>13</sup> The length of the reference cavity is 45 cm. The mirrors have a radius of curvature of 228 mm that ensures all low-order transversal modes to be further than 40 MHz away from any longitudinal mode. The finesse of the cavity is 300. One of the mirrors sits on a PZT mounting, allowing the cavity resonance frequencies to be scanned. For a perfectly working stabilization, the cavity on which the laser frequency is locked defines the stability of the laser. It is therefore essential to guarantee good stability for the cavity modes, i.e., to protect them from mechanical, acoustic, and thermal noise. The cavity rod was made of Invar and was sustained inside a vacuum chamber.

As shown in Fig. 4, a part of the laser light was

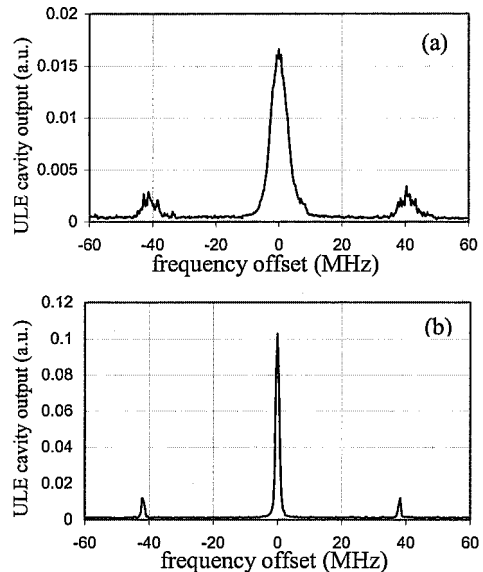


Fig. 5. Transmitted intensity through the supercavity versus the frequency offset between a resonant frequency of the supercavity and the laser frequency when (a) the laser frequency is unlocked and (b) the laser frequency is locked to a resonant frequency of an  $F = 300$  cavity.

focused through an electro-optic modulator driven by a 40-MHz radio frequency that phase modulates the transmitted light. We observed the typical dispersion line shape given after demodulation by the signal reflected by the cavity.<sup>13</sup> We adjusted the necessary quadrature of the demodulated signal by simply varying the length of the signal-carrying wires. This typical line shape has a steep central slope, which ensures a fast response to laser frequency fluctuations and is quite suitable as a frequency discriminator. The adjacent slopes are 40 MHz apart, so that the locking range is quite large. The error signal was fed back to the elements that control the laser frequency. A frequency switch separates the fast fluctuations ( $>100$  Hz), which are fed directly to the laser current control from the slow fluctuations ( $<100$  Hz), which are fed to the PZT that controls the translation of the grating in the extended cavity setup. The bandwidth of our feedback loop is currently limited by the bandwidth of the commercial laser diode current drive, which is approximately 100 kHz. To increase the bandwidth, one would have to bypass this current drive and to supply the diode directly.

We can evaluate the upper limit for the bandwidth of our laser by simply measuring its frequency resolution on a transmission curve of an independent supercavity with a finesse superior to 15,000 and a fixed length of 10 cm. This technique provides a somewhat absolute measure of the laser linewidth. Figure 5 shows the transmission spectrum of the output of the supercavity by scanning the diode laser longitudinal mode. In Fig. 5(a) we scanned the extended cavity setup by translating the grating, whereas in Fig. 5(b) we locked the diode laser to the

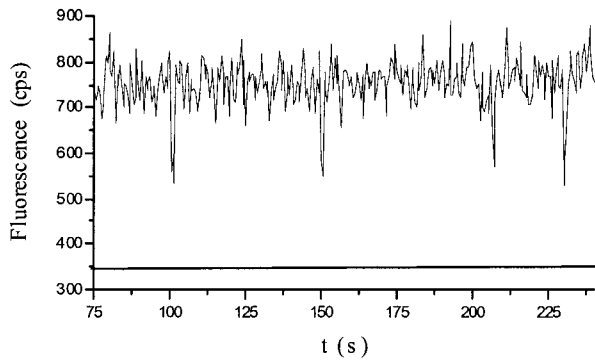


Fig. 6. Quantum jumps driven by the diode laser observed on two ions stored in a Paul–Straubel trap. The upper level corresponds to the fluorescence of two ions at 397 nm, the lower level is the fluorescence of only one of the two ions. The line at approximately 350 counts/s corresponds to stray light.

reference cavity and the length of the reference cavity was swept. The tiny sidebands at  $\pm 40$  MHz resulted from the electro-optic phase modulation and serve to calibrate the frequency axis. These curves were averaged over 64 scans and the duration of each was 140 ms with a 0.5-ms resolution. From these curves, the measured linewidth for the unlocked laser is 6.2 MHz. For the locked laser, the linewidth is inferior to 500 kHz. This remaining linewidth is principally due to mechanical and thermal noise of both the reference and the supercavities.

## 5. Resonance Excitation in Ions

The laser was used to drive the  $4S_{1/2}-3D_{5/2}$  electric quadrupole transition of  $\text{Ca}^+$  ions stored in a radio-frequency trap. This forbidden transition has a relaxation rate of approximately 1 photon/s and therefore does not allow direct observation of fluorescence scattering. However, by use of Dehmelt's quantum amplifier scheme,<sup>14</sup> it was possible to monitor each single excitation process with a single ion by means of the sudden breakdown of the fluorescence from the simultaneously driven strong dipole transition. This random switching is the signature of quantum jumps. The quantum jump rate, depending on the excitation parameters such as laser intensity and detuning, forms the reference signal for locking the clock laser.

Ions have been confined and laser cooled in a miniature Paul–Straubel trap.<sup>15</sup> Some hundreds of microwatts of the 729-nm diode laser have been focused onto the trapped particles, which was enough to induce quantum jumps. In this case, the fluorescence count rate for a single ion is approximately 200 counts/s with an overall scattered background of approximately 350 counts/s. The latter is due mainly to the scattering of the cooling laser at 397 nm. Figure 6 shows some of the quantum jumps of one ion observed on an ensemble of two ions.

## 6. Conclusion

To improve its spectral and spatial behavior, we set up a broad-area diode laser in an external cavity.

Single-mode output has a width of approximately 8 MHz and its transverse profile is nearly Gaussian and circular. This laser was stabilized with a low-finesse reference cavity within the range of a few hundred kilohertz. This linewidth reduction was obtained at the cost of a reduction in the useful optical power left for experimentation, which justifies the use of high-power semiconductor components. The diode laser we have presented constitutes a compact system that can be used to drive the clock transition of a proposed  $\text{Ca}^+$  atomic clock in the optical range.

For future experiments, when ion cooling is sufficient to reach the Lamb–Dicke regime, the first-order Doppler effect would be discrete and the linewidth of the quadrupole resonance would drop to a value inferior to 1 kHz. To adjust the laser linewidth to the potential of the clock transition, it must be narrowed further. We intend to reduce the laser frequency fluctuations by increasing the feedback servo bandwidth and then by stabilizing the laser to a high-finesse cavity ( $F > 15,000$ ). The mirrors of this second cavity are optically contacted on the spacer that is made of ultralow expansion (ULE) material. This cavity must be well isolated from mechanical, acoustic, and thermal fluctuations. Dye or solid-state lasers have already been stabilized in this way under the 1-Hz level.<sup>16</sup> Single-mode diode lasers have been stabilized under the 10-Hz level,<sup>17</sup> which limit we aim to reach with broad-area diode lasers.

## References and Note

1. A. Bauch and H. R. Telle, "Frequency standards and frequency measurement," *Rep. Prog. Phys.* **65**, 789–843 (2002).
2. M. Knoop, M. Vedel, and F. Vedel, "Lifetime, collisional-quenching, and  $j$ -mixing measurements of the metastable  $3D$  levels of  $\text{Ca}^+$ ," *Phys. Rev. A* **52**, 3763–3769 (1995).
3. P. A. Barton, C. J. S. Donald, D. M. Lucas, D. A. Stevens, A. M. Steane, and D. N. Stacey, "Measurement of the lifetime of the  $3d\ ^2D_{5/2}$  state in  $^{40}\text{Ca}^+$ ," *Phys. Rev. A* **62**, 032503 (2000).
4. F. Neudel, S. Takatani, H. Reul, and G. Rau, "Effect of hemolysis on oxygen and hematocrit measurements by near infrared reflectance spectroscopy," *Med. Eng. Phys.* **24**, 301–307 (2002).
5. For more information see <http://www.appliedoptronicscorp.com>.
6. M. W. Fleming and A. Mooradian, "Spectral characteristics of external-cavity controlled semiconductor lasers," *IEEE J. Quantum Electron.* **QE-17**, 44–59 (1981).
7. A. Mooradian, "Cavity controlled semiconductor lasers," *IEEE J. Sel. Top. Quantum Electron.* **6**, 1318–1324 (2000).
8. T. Pawletko, M. Houssin, M. Knoop, M. Vedel, and F. Vedel, "High power broad-area diode laser at 794 nm injected by an external cavity laser," *Opt. Commun.* **174**, 223–229 (2000).
9. G. L. Abbas, S. Yang, V. W. S. Chan, and J. G. Fujimoto, "Injection behavior and modeling of 100 mW broad area diode lasers," *IEEE J. Quantum Electron.* **24**, 609–617 (1988).
10. R. J. Lang, D. Mehuys, D. F. Welch, and L. Goldberg, "Spontaneous filamentation in broad-area diode laser amplifiers," *IEEE J. Quantum Electron.* **30**, 685–694 (1994).
11. M. Houssin, B. Fermigier, and M. Desaintfuscien, "Simulation of the frequency behavior of external-cavity semiconductor lasers," *IEEE J. Quantum Electron.* (to be published).

12. P. Zorabedian, W. R. Trutna, and L. S. Cutler, "Bistability in grating-tuned external-cavity semiconductor lasers," *IEEE J. Quantum Electron.* **QE-23**, 1855–1987 (1987).
13. R. W. P. Drever, J. L. Hall, F. V. Kowalski, J. Hough, G. M. Ford, A. J. Munley, and H. W. Ward, "Laser phase and frequency stabilisation using an optical resonator," *Appl. Phys. B* **31**, 97–105 (1983).
14. H. G. Dehmelt, "Proposed visual detection laser spectroscopy on single Ba<sup>+</sup> ion," *Bull. Am. Phys. Soc.* **20**, 60–62 (1975).
15. C. Champenois, M. Knoop, M. Herbane, M. Houssin, T. Kaing, M. Vedel, and F. Vedel, "Characterization of a miniature Paul–Straubel trap," *Eur. Phys. J. D* **15**, 105–111 (2001).
16. B. C. Young, F. C. Cruz, W. M. Itano, and J. C. Bergquist, "Visible lasers with subhertz linewidths," *Phys. Rev. Lett.* **82**, 3799–3802 (1999).
17. C. H. Shin and M. Ohtsu, "Stable semiconductor laser with a 7-Hz linewidth by an optical–electrical double-feedback technique," *Opt. Lett.* **15**, 1455–1457 (1990).